28 pages

GRANT/GODDARD

FINAL REPORT

NASA GRANT # NAG 5-556

Ultraviolet Observations of Astronomical Phenomena

CR

IN-26384

Period of Grant

June 15, 1985--June 14, 1986

Principal Investigator

Dermott J. Mullan

Bartol Research Foundation

University of Delaware

Newark, Delaware 19716

September 9, 1986

Final report for NASA Grant NAG 5-556

D. J. Mullan

Bartol Research Foundation of the Franklin Institute, University of Delaware, Newark DE 19716

1. Introduction

The purpose of this research was to study various aspects of mass loss in stars of different types. The observational part of the research was directed at three Cepheid variables; the archival part of the research was directed at hot stars (for information on corotating interaction regions) and at cool giants (for study of variability in the mass losing part of the atmosphere).

2. IUE Observing

This work is being done in collaboration with a European astronomer (H. Deasy, Dunsink Observatory, Ireland), who obtained observing time at Vilspa. One US2 shift was awarded to obtain high resolution spectra of the MgII h and k lines in Cepheids to search for highly shifted absorption components, such as might occur if mass loss is episodic in these variables. My collaborator and I agreed that we would be responsible for obtaining spectra of certain Cepheid variables at distinct phases of their pulsation, so as to provide as much phase coverage as possible. For L Carinae, I was assigned the phase range 0.5-0.8; for Beta Doradus, I was assigned the phase range 0.7-1.0(0.0); and for Zeta Geminorum, I was assigned the phase range 0.9-1.2 (0.2).

Finding charts were generated for all three stars using STARLINK software during my appointment as a Visiting Scholar at Dunsink Observatory in August-September 1985. The finding charts are complete down to magnitude 11. Charts were generated for various equinoxes and for various sizes of areas around the target star, from 5X5 sq.arcmin., to 20x20 sq. arcmin (as an example, see Fig. 1). Each chart is accompanied by a list of the stars in the plotted area, including HD number, BD number, spectral type, B and V magnitudes, position (to 0.1 sec of RA and 1" of Dec), and offset from the target star. The advantage of having software to plot finding charts is very great: I am not aware of any such capability in the USA. But it would be a useful addition to IUE users if the RDAF could have such software on line.

Ephemerides of the three stars were generated, based on periods and epochs in the literature. The periods of the three stars are highly noncommensurate (35.533, 9.84295, and 10.1535 days, respectively). Thus, in the space of one IUE funding year (starting May 1, 1985), the windows during which all three stars fall within the appropriate intervals of phase in their pulsation, are narrow. The first such window after May 1 was Nov. 5-6, 1985; other windows occured on Dec. 14-17, 1985, Jan. 14-16, 1986, Feb. 24, 1986, and March 26, 1986. Of these, not all were suitable for IUE observing because of unfavorable beta angles of the spacecraft. We were successful in being scheduled for the first window, but not for any of the other windows. Thus, our second observing run entailed a compromise on the phase of L Carinae.

The shift was split in two. On Nov. 5-6, 1985, spectra were obtained of L Carinae at phase 0.60, and Beta Doradus at phase 0.77; On April 15, 1986, spectra were obtained of L Carinae at phase 0.14, Beta Doradus at phase 0.01, and Zeta Geminorum at phase 0.90.

On Nov. 5-6, we obtained a 55 minute exposure (LWP 7049) of L Carinae, when its FES magnitude was 4.4. In the Mg h and k lines, the maximum DN

counting rates were 108. Thus, this image is somewhat underexposed for the purposes of searching for absorption components in the nearby continuum. We also obtained a 38 minute exposure (LWP 7050) on Beta Doradus (FES magnitude 3.9). Because of long slew times at the start of this half-shift, we were not able to obtain a spectrum of Zeta Geminorum at all.

On April 15, 1986, L Carinae had an FES magnitude of 3.6. A 50 minute exposure (LWP 8034) yielded a maximum DN counting rate of 209 in Mg h and k emission. For Beta Doradus, with FES magnitude 3.6, a 30 minute exposure (LWP 8033) yielded maximum DN counting rates of 138 in Mg emission. For Zeta Geminorum, with FES magnitude 3.7, a 48 minute exposure (LWP 8035) yielded maximum counting rates of DN=185.

My collaborator obtained two half shifts at Vilspa on October 24 and December 4, 1985. On the first half shift, he obtained two HIRES LWP: Beta Doradus at phase 0.5, and L Carinae at phase 0.3. On Dec. 4, he obtained Zeta Gem at phase 0.8 and T Vul at phase 0.2. Thus, our observing data cover different phases of the three stars which are common to both of our samples.

When the NASA data tapes were available from the first run, I used standard reduction software at the IUE RDAF at Goddard to extract flux profiles of Mg II h and k lines. Abscissae were converted to a nominal velocity scale using the rest wavelengths of both lines, 2796.347 and 2803.523A. The fluxes were plotted on velocity scales from -300 to +200 km/sec. These were then smoothed with various degrees of smoothing, from 3-point to 20-point smoothing. In Fig. 2 we show examples of smoothed velocity profiles for both h and k lines in LWP 7050, Beta Doradus. In Fig. 3, we show examples of smoothed velocty profiles for both h and k lines in LWP 7049, L Carinae. In both figures, histograms refer to the h line, while continuous lines refer to the k line profile. The resulting h and k line profiles are used as input by my collaborator to model the gross velocity field in the atmosphere of the Cepheid: he chooses a velocity field as a function of altitude which is meant to be representative of the state of pulsation at the appropriate phase, and then computes the h and k profiles using a partial redistribution NLTE code (originally developed at NCAR by J. Linsky et al.) The velocity field may be non-monotonic Our smoothed h and k profiles allow the velocity field in the regions of the atmosphere where the Mg h and k emission components are formed to be determined as a function of phase.

The qualitative differences between the smoothed profiles in the three stars of our sample are striking, even to the eye. Thus, Beta Doradus, on Nov. 5-6, 1985, (at phase 0.77) showed a prominent double emission feature in both h and k, with peaks at +(10-30) and -(160-180) km/sec. and with the ratio of blue/red emission peaks of about 0.6 (see Fig. 2). However, on April 15, 1986, at phase 0.01, the profile was entirely different: now, only a single emission peak was present, centered close to zero velocity. The blue peak was entirely absent, with a ratio of certainly no more than 10% of the "red" peak (see Fig. 4 for 5-point smoothed profile). This drastic alteration in the overall appearance of the h and k emission feature in Beta Doradus in the space of 160 days (perhaps due to different phases) indicates that the atmospheric velocity field in the regions where h and k are formed underwent gross alterations. Somehow, the blue emission has been completely absorbed (or suppressed) in the second exposure.

Qualitatively different behavior was observed in L Carinae. Here, in the first exposure, a "red" peak occurred around velocity zero, and a "blue" peak at about -150 km/sec. The ratio of peak emission fluxes in blue and red peaks was about 0.6 for the k line, and about 0.8 for the h line (see Fig. 3). In the second exposure (160 days later), at phase about 180 degrees away from the first exposure, the blue emission in the k line had strengthened to have almost exactly

the same peak flux as the red emission, while the h-line retained essentially the same value for blue/red peak flux ratio (see Fig. 5 for 7-point smoothed profile). Thus, there is no sign of drastic suppression of blueward emission in L Carinae in our data.

In Zeta Geminorum, the one spectrum which we obtained shows a blue emission peak at about -150 km/sec, and a red peak at about zero velocity (see Fig. 6 for 5-point smoothed profile). Thus, the velocity structure of the peaks appears quite similar to those in L Carinae. However, an interesting difference is that in Zeta Geminorum, not only is there no suppression of the blue peak, but the blue peak is actually stronger (at peak flux) than the red peak (by at least 10%). This would be quite an unusual spectroscopic signature in a star which is losing mass at a rapid rate. Thus, Zeta Geminorum apparently is not a heavy mass-loser.

Detailed modelling of our new profiles for all three stars will impose tighter constraints on the velocity fields in their atmospheres at the appropriate pulsation phases.

Although pulsation is a well known characteristic of Cepheids, it is not yet known whether mass loss accompanies the pulsation. Pulsation might be expected to yield time-dependent mass loss, with associated discrete spectral signatures. We therefore wish to search for possible spectral features lying at the same velocity in both h and k lines. The reality of an absorption (or emission) feature in the profile of, say, the h line is suspect if no absorption (or emission) feature of appropriate strength appears at the same velocity in the k line. By "appropriate strength", we mean that the equivalent width of the absorption (or emission) feature in k should be greater than that in the h line by a factor of up to 2 (in the limit of small optical depth).

Notice that because we have used the rest wavelength of both lines for purposes of conversion from wavelength to radial velocity, without allowing for radial velocity effects due to stellar motion, stellar pulsation, or satellite motion, the velocity scale on any one LWP spectrum is only relative. However, this is of no consequence as far as identifying the reality of common absorption features in h and k.

To put our comparison of the h and k profiles on a quantitative basis, we used the routine RV in the IUE RDAF to extract radial velocities for every peak and dip in the (unsmoothed) k line between 2792 and 2800 A, and for every (emission) peak and (absorption) dip in the (unsmoothed) h line between 2800 and 2808 A. These correspond to velocity ranges of about -400 to +400 km/sec. The escape velocity from the surface of a Cepheid is much less than 400 km/sec (typically 100-200 km/sec), so that if a blue shifted feature is found at -400 km/sec, it is certainly not bound gravitationally to the star. On the other hand, it is also of interest to explore the redward side of zero velocity, because of possible infalling material.

In L Carinae (LWP 7049), some 50-60 peaks and dips were measured in both profiles. Some of these are undoubtedly noise. To decide on the real features, a routine was written to compare the radial velocity table of all peaks in the k line with all peaks in the h line, and the same with the dips in both lines. We ask the question: how many peaks and/or dips coincide in velocity within a particular tolerance, dv? With dv=+-1 km/sec, eight peaks and 6 dips coincided in the h and k lines. With dv=+-2 km/sec, the coincidences grew to 14 and 10 respectively. The sampling interval between points in the extracted IUE spectra is 5 km/sec. Thus, with dv=+-2 km/sec, we are almost covering the distance between adjacent sampling points. The 14 emission coincidences occur at -365, -354, -309, -261, -244, -150, -129, -80, -22, and -11 km/sec on the blueward side of

line center, and at 53, 101, 148, 378, and 405 km/sec on the redward side. The first five of the emission peak coincidences certainly lie at super-escape velocities, and hence represent mass loss events if they are real. For the 10 absorption dip coincidences, the most blueward components occurred at -359, -335, and -313 km/sec.

My collaborator, in his spectrum of L Carinae obtained on October 24 (i.2. 12-13 days earlier than mine), has concluded that "at least one significant absorption was present in the L Carinae spectrum at a blueshift of less than -250 km/sec". Referring to earlier work by Schmidt and Parsons (at different phases), and noting that my spectra also contain blueshifted absorption dip coincidences at less than -250 km/sec, he concludes that "at least one high velocity blueshifted absorption component faster than the escape speed persists for a large fraction of a pulsation cycle" (letter dated July 11, 1986).

In view of these remarks, it was a matter of some interest to see whether coincident dips would appear in velocity space for both h and k lines in the spectrum of L Carinae obtained April 15, 1986. With a tolerance of dv=+-2 km/sec, dips coincide at -367, -332, -274, -209 km/sec (as well as at other velocities, less than escape speed). Again, the appearance of coincident dips in the spectrum at less than -250 km/sec is striking, particularly since velocities of the two most blueshifted dips are quite close to those detected on November 5-6, 1985, some 160 days earlier. Thus, over a time span of almost 5 pulsation cycles, coincident dips appear in the h and k lines at essentially the same velocity. Unfortunately, the signal/noise ratio at these large blue-shifts is not sufficient to determine accurately the ratio of equivalent widths of the absorption features in h and k. Deeper exposures will be needed in order to evaluate this ultimate test of the reality of the dips which coincide in velocity in h and k.

For Beta Doradus, the same procedure was applied to LWP 7050 and LWP 8033. With dv=+-2 km/sec, the first spectrum showed 14 coincident emission peaks and 12 coincident absorption dips in h and k. Of the dips, those at -328, -316, -306, -251, and -187 km/sec are candidates for escaping matter. On the second spectrum, coincident dips were found at -319, -272, -202, and -160 km/sec (in the super-escape regime). Again, the persistence of a coincident dip at about -317 km/sec over a 160 day interval may indicate long-lived mass-losing structure in the surroundings of Beta Doradus. Dr Deasy remarks that he has not been able to identify with confidence any components in his Beta Doradus spectrum solely on the basis of inspection of the calcomp plots with which he was provided.

For Zeta Geminorum, coincident dips appeared in h and k (within dv=+-2 km/sec) at -395, -196, and -110 km/sec. No information is yet available about temporal variability of these dips in Zeta Geminorum. Dr Deasy has so far inspected only the calcomp plots of his spectrum of Zeta Geminorum, and from these, he has not yet confidently identified any absorption components.

3. IUE Archival Studies

When stars lose mass in a non-spherically symmetric manner, the possibility arises of forming "co-rotating interaction regions" (CIRs) in the wind, where fast wind catches up with slower wind. The velocity structure of the wind in such a case includes a plateau, bordered by forward and reverse shocks. The spectral signature of the plateau is a narrow absorption component superposed on an overall P Cygni profile. Because of the heating associated with the shocks, the material in the plateau is expected to be weighted in favor of more highly ionized species. As a result, we have been searching in stars of various spectral types for such CIR signatures in the profiles of SiIV, NV, and CIV.

We have used high resolution SWP images of Delta Ori (O9 II), Mu Nor (B0 I), Rho Leo (B1 I), and Xi Per (O7 III) to extract the profiles of the above three lines in all available exposures. To date, we have extracted 341 line profiles, which are now available as .SAV files in my disk area on the IUE RDAF PDP-11. All show the typical P Cygni profile as a prominent feature. As examples, we show in Fig. 7, the profiles of NV, SiIV, and CIV in SWP3031 for Xi Per. However, as well as the usual P Cyg profiles, superposed on certain exposures, narrow absorption dips are also present, displaced to large negative velocities. These displaced narrow components (DNCs) are, we believe, good candidates for CIR's. Arguments in favor of this belief are presented in the attached manuscript, which is now in press in Astronomy and Astrophysics.

Before analyzing the DNC's themselves, we must first remove the effects of the background P Cygni profile. To do this, we have used the program COMPAR at the IUE RDAF at Goddard. As input for this program, we first must normalize our .SAV files of the various line profiles to the continuum, using the GNORM procedure on RDAF.

The COMPAR routine computes a P Cyg profile in terms of the parameters of the optical depth distribution and the velocity profile of the wind. The velocity profile (assumed to be spherically symmetric) is parameterized by a terminal velocity and by an exponent beta which characterizes how rapidly the velocity approaches terminal value: small beta represents a more slowly accelerating wind than large beta. The optical depth is parameterized by an amplitude plus an exponent (which characterizes how rapidly the optical depth grows as velocity approaches terminal. For doublets such as we are using), the amplitude of the shortward component must be specified as double that of the longward component. Photospheric absorption lines must also be allowed for in some of the hotter stars in order to obtain a good fit.

The aim is to find a unique velocity law which fits all three doublet profiles. Terminal velocity is easiest to extract, and the NV line seems to be the best line to start with in order to determine the best choice of velocity law. Then, switching to the SiIV and CIV lines, one attempts to fit their P Cyg profiles by varying only the optical depth parameters.

As examples, we discuss here, three SWP images which we have fitted by COMPAR: SWP 1859 (Rho Leo), SWP 3035 (Xi Per), and SWP 4018 (Delta Ori). For Rho Leo, the NV doublet was fitted best by terminal velocity of 1500 km/sec (see Fig. 8). A velocity exponent of 4 seemed to work best for the NV line. Rather weak photospheric absorption was required for a good fit: central depths of 0.2 and 0.1 for blue and red lines. This velocity law then leads to quite a good fit of the CIV profile in the same spectrum, provided that the amplitude of the opacity in the CIV lines is chosen to be some 6 times larger than in the NV lines (see Fig. 9). Finally, we switch to the SiIV lines (which are always the hardest to fit because of the wide separation of the doublet components, 1393.75 and 1402.77 A). These lines could be fitted reasonably well with the same velocity parameters, and an amplitude for the optical depth smaller by a factor of about 2 than for CIV (see fig. 10).

For Xi Per, a terminal velocity of 3800 km/sec seemed to fit best, again with a velocity exponent of 4 (i.e. a rapidly accelerating wind). Very strong CIV absorption is present, requiring amplitudes for the opacity some 4 times greater than in Rho Leo. Also, in order to fit the emission side of the profile, strong photospheric absorption was necessary in CIV (central depths of absorption 0.9 and 0.45) (see Fig. 11). With these combinations, the emission side of the profile was fitted very well.

For Delta Ori, the terminal velocity was found to be 2600 km/sec, and a slower accelerating flow (beta=2) was found best. Rather strong photospheric absorption again was needed (central depths of 0.8 and 0.4 in CIV) (see Fig. 12). However, in this case, the amplitude of the optical depth in the wind was quite small compared with that in Rho Leo, smaller by a factor of 6. Thus, either the mass loss rate from this star is considerably smaller than that from Rho Leo, or else, something is reducing the amount of carbon in the form of CIV in the wind. In this star, the SiIV doublet required again an opacity amplitude in the wind intermediate between that for CIV and that for NV. Thus, the relative abundances of CIV, SiIV, and NV appear quite similar in the cases of Delta Ori and Rho Leo.

However, in the case of Delta Ori, there is a very strong absorption dip in the SiIV profile which cannot be reproduced by the P Cygni calculation (see Fig. 13). A DNC at -1800 km/sec has been reported in this star by Prinja and Howarth (ApJSuppl, 1986, in press), and this may be why the P Cyg profile fitting does not work well in this case. For quantitative modelling of the DNC's, the background P CYg profiles must first be fitted rather well, and then subtracted off to leave the remnants of DNCs to be modelled separately.

To help identify DNC's more readily, we have performed differencing of one spectrum of a star relative to a spectrum at a later time. We convert the spectrum of a particular line profile to a velocity scale, and then do point-by-point subtraction of two images. For example, for the star Mu Nor, we converted the CIV profiles to velocity scales in exposures SWP 21003 and 21051 (taken 4 days apart in September 1983). Then, plotting on a velocity scale from -4000 to +4000 km/sec, we plotted the difference (see Fig. 14). Over most of the velocity range, the differences lie in the noise. But at -1900 km/sec, an obvious change has occured in the course of the 4 days between exposures. A lesser change is also apparent at -2200 km/sec. There are also changes in the vicinity of zero velocity. By taking advantage of the smoothing properties of IDL, and the various plotting routines, the differences between different images can be highlighted so as to enhance the detectability of variable features. In Mu Normae, prominent DNC's have been reported in earlier exposures (prior to, and including, 1982 July 10) by Prinja and Howarth, at velocities of -1600 to -2000 km/sec. Thus, it is likely that our differencing technique has indeed led to identification of a bonafide DNC in the more recent exposures of this star. Complete modelling of the P Cygni profiles of this star is required first before properties of the DNC's can be reliably extracted. However, it is clear that we have been able to identify reliably the candidates for DNC's in some of the stars in our sample.

A second aspect of the archival research concerns the variations of UV line fluxes at various levels of the atmosphere of cool giants. The aim is to search for rotational modulation and also to follow events of mass loss as they proceed from the lower levels of the atmosphere upwards. Our earlier evaluations of rotational velocities in 8 stars using archival measurements of the Mg h and k emission fluxes have been checked recently in an independent spectroscopic study by D. Gray. Seven of the stars in our sample were in Gray's sample. He derived values of v sin i which, when corrected by an average value of sin i = pi/4 led to values of equatorial rotational velocuty which were in excellent agreement with ours in 4 of the 7 stars. In two others, the value required for sin i to bring Gray's value of v and ours into agreement are smaller than the average value of pi/4 by factors of about 2. However, a random distribution of sin i values leads to the expectation that such smaller values of sin i would be expected to occur with a frequency such that indeed, in Gray's sample of stars, at least one or two stars should have been detected in that range of sin i. Thus, six of the seven stars seem acceptable in their agreement. The only exception was Theta Herculis,

(Ap. J., in press)

where the required value of sin i to bring ours and his results into agreement is so small as to be rather unlikely, although not impossible.

In all cases, it is noteworthy that Gray's values of v sin i are all less than our estimates of v. It would have been impossible to reconcile our results with his if he had found a case where his v sini value exceeded our estimate of v. Thus, our rotational modulation method using archival Mg II h and k fluxes seems to be quite reliable. Several recent exposures of some of our target stars have been taken by A. Brown and collaborators with the precise purpose of checking our rotational modulation predictions. We are now waiting to have these exposures released to check our earlier predictions of the periods of rotation.

My ex-graduate student, Dr. Jeffrey Brosius, now at Goddard Space Flight Center, is currently involved on a part-time basis on this aspect of the archival research, using the IUE RDAF.

Attached: 14 Figures
1 manuscript (6 pages)

STARCHART ZETA GEM
CENTRE : 07 01 09 , +20 38.0 (1985.0)
EPOCH : 1950.0

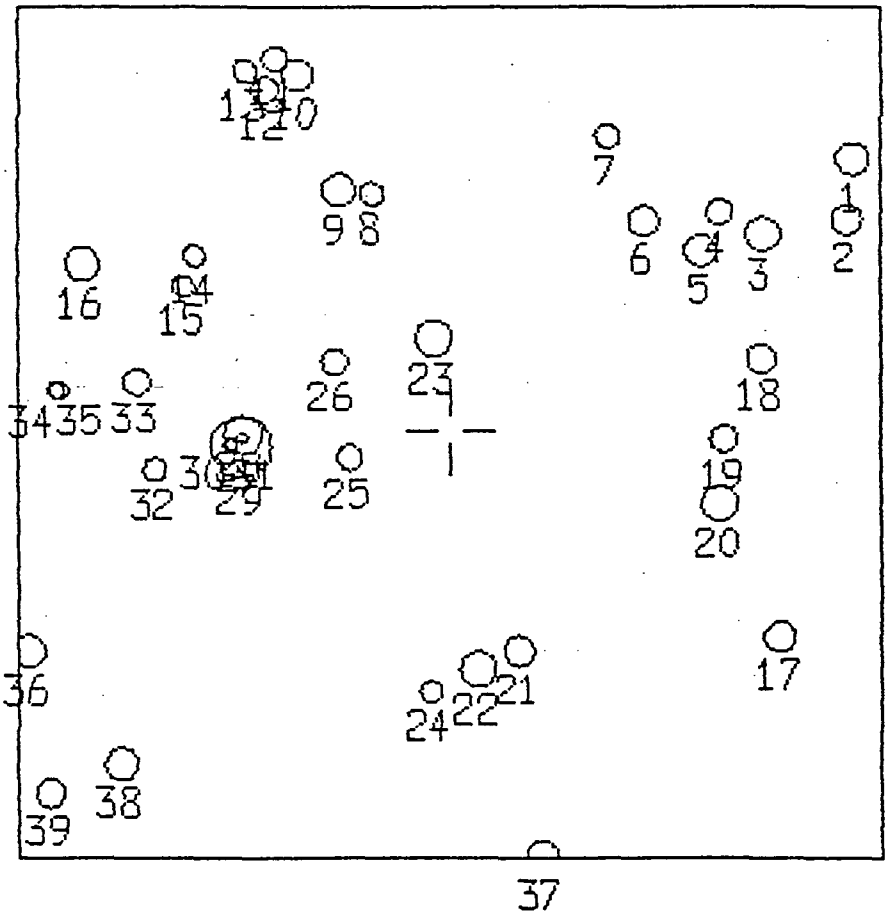

MAGNITUDES
4
5
6
7
8
9
10
11

20'
SQUARE

Fig. 1

histo = h-line (2)
smooth = k-line

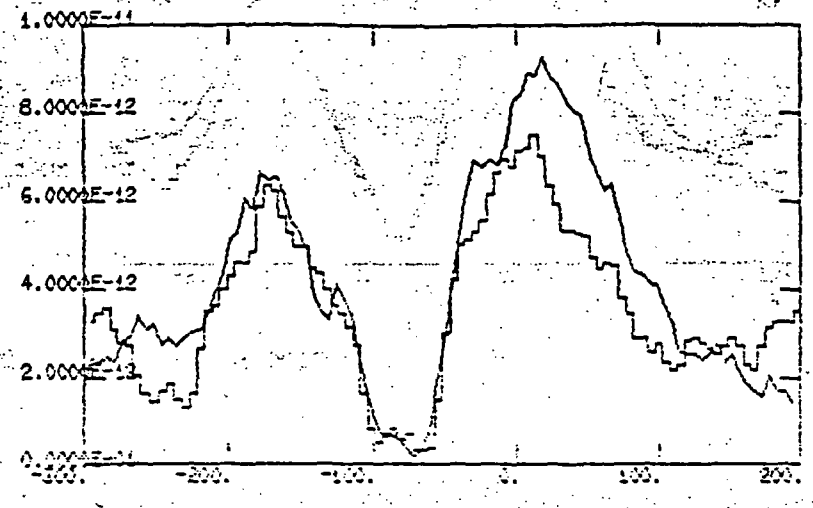

IDL>!PSYM=10 & OPLOT,V2,SMOOTH(F,5)

3 point smoothing

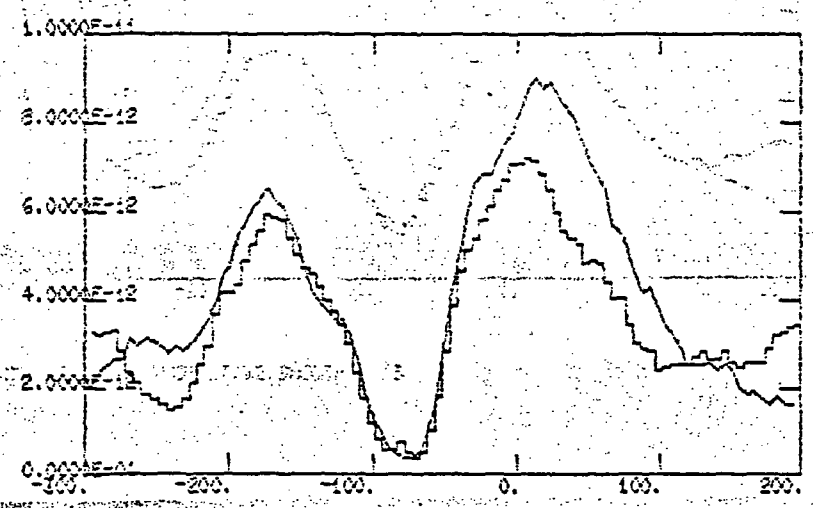

IDL>!PSYM=0 & OPLOT,V1,SMOOTH(F,7)

5-point

7-point

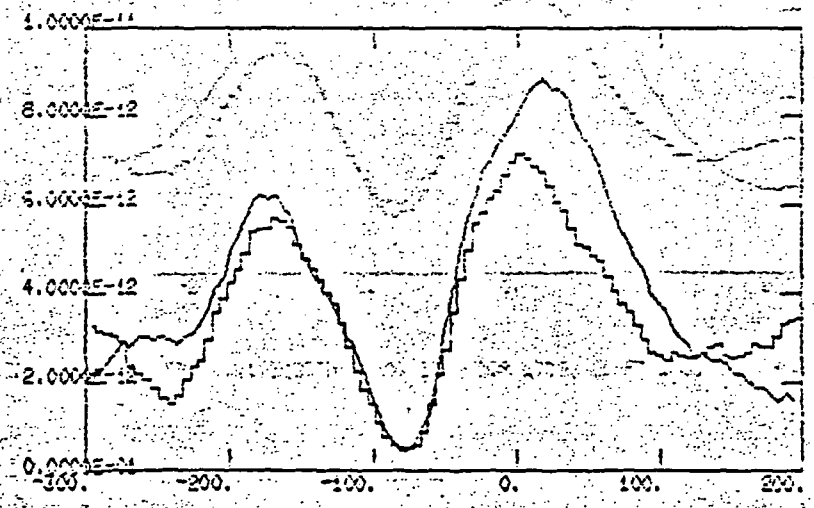

IDL>!PSYM=10 & OPLOT,V2,SMOOTH(F,9)

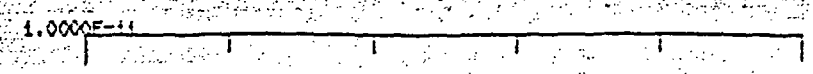

Fig. 2
Smoothed profiles
h+k lines
Mg II
LWP 7050
β Dor

smoothed 4th line
L Carinae
LWP 7049

IDL>!PSYM=10 & OPLOT,V2,SMOOTH(F,5)

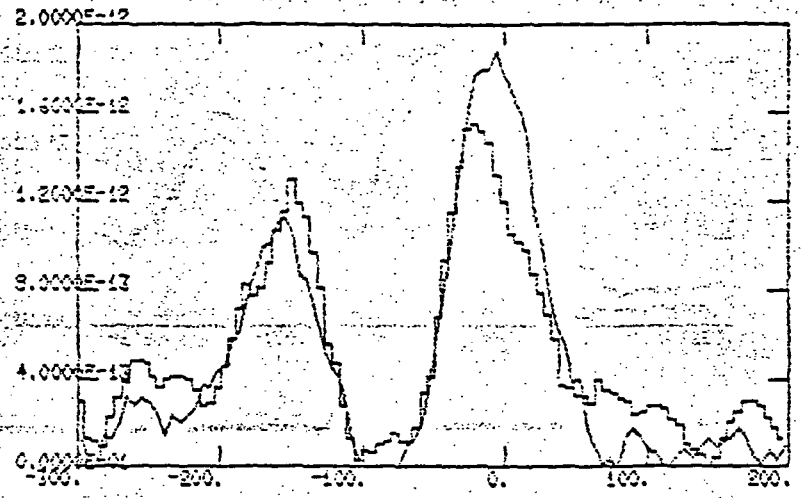

5 point smoothing

IDL>!PSYM=0 & OPLOT,V1,SMOOTH(F,7)

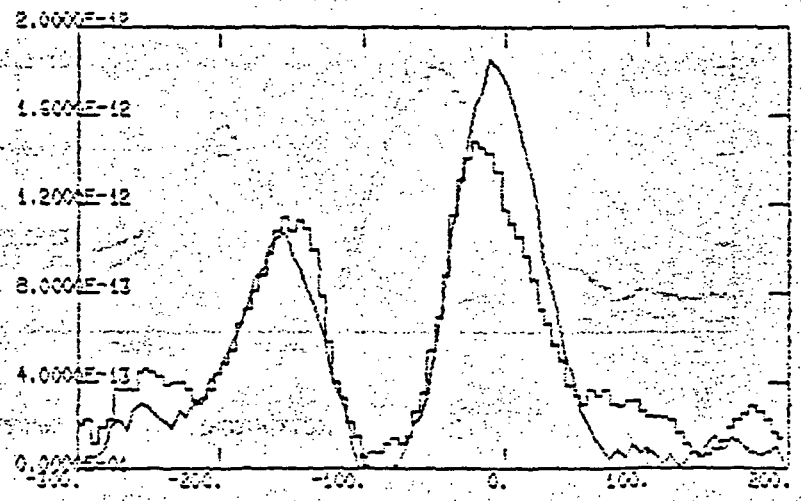

7-point

hist=h line
contin=k line

IDL>!PSYM=10 & OPLOT,V2,SMOOTH(F,9)

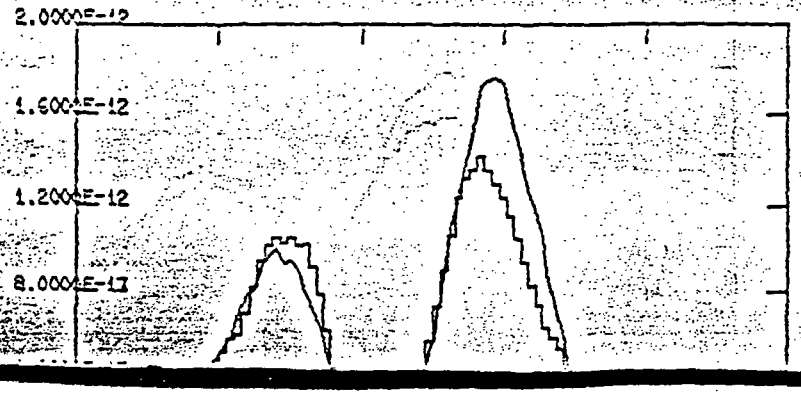

FIG 3

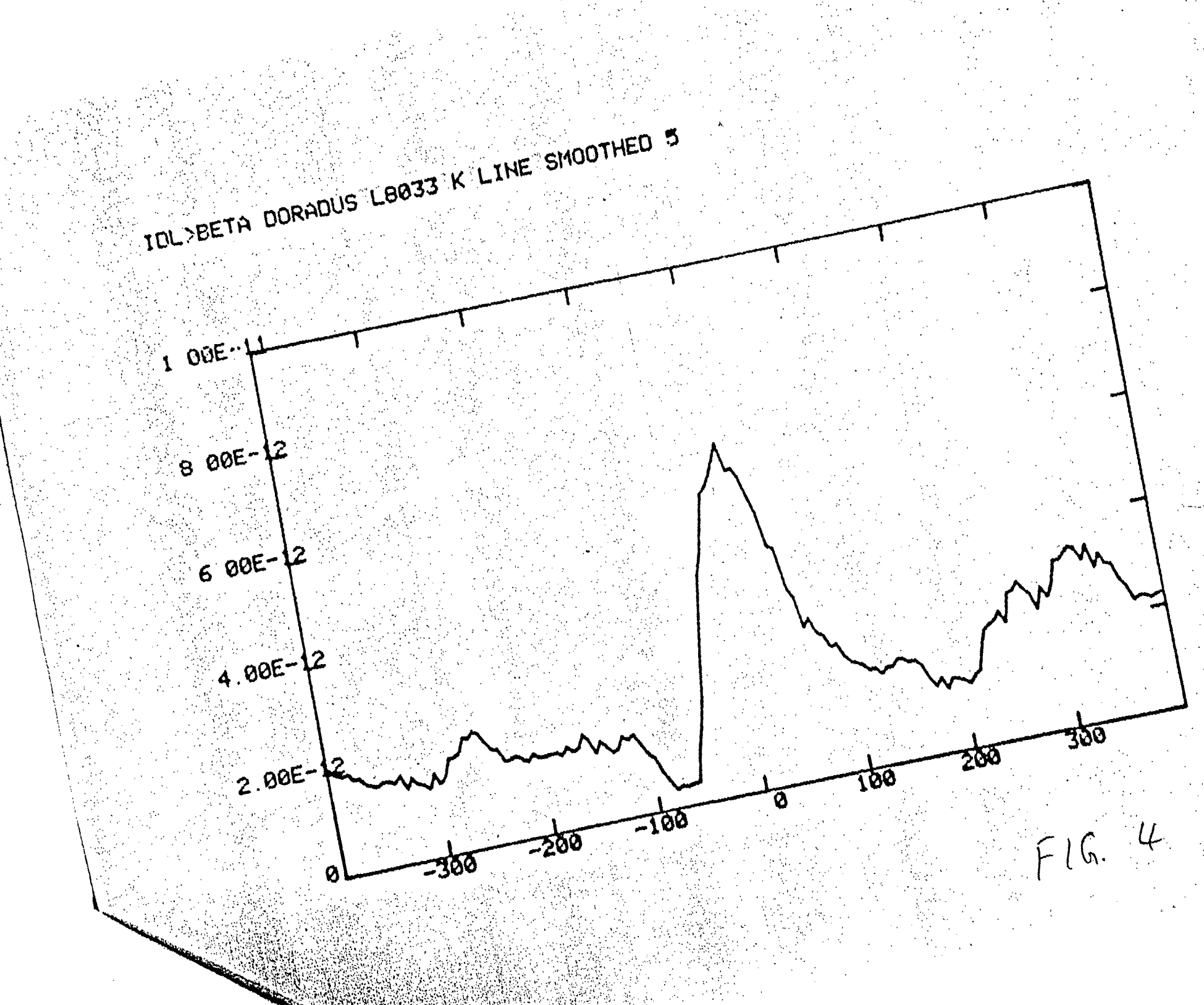
IDL>BETA DORADUS L8033 K LINE SMOOTHED 5
1.00E-11
8.00E-12
6.00E-12
4.00E-12
2.00E-12
0
-300
-200
-100
0
100
200
300

FIG. 4

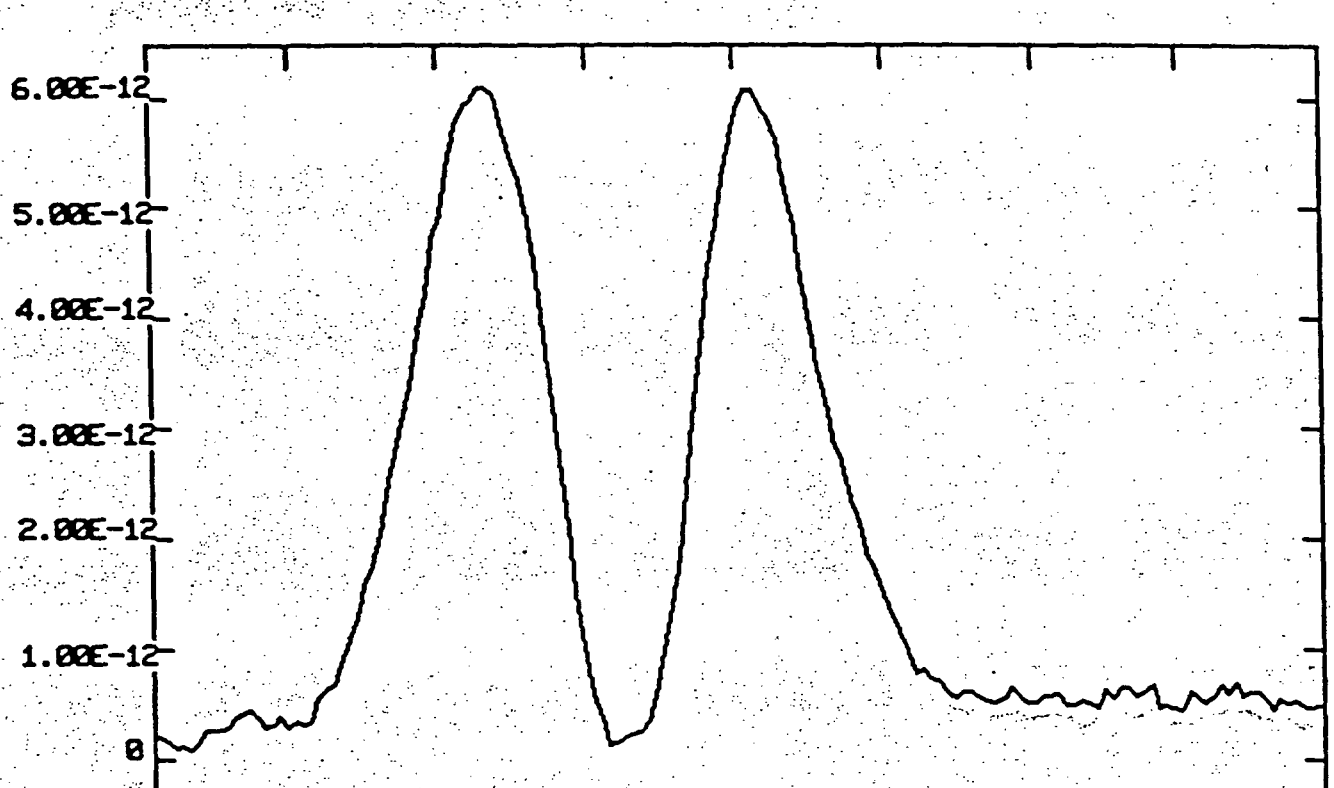
IDL>L CARINAE L8034H K LINE SMOOTH 7
6.00E-12
5.00E-12
4.00E-12
3.00E-12
2.00E-12
1.00E-12
0
-300
-200
-100
0
100
200
300

FIG. 5

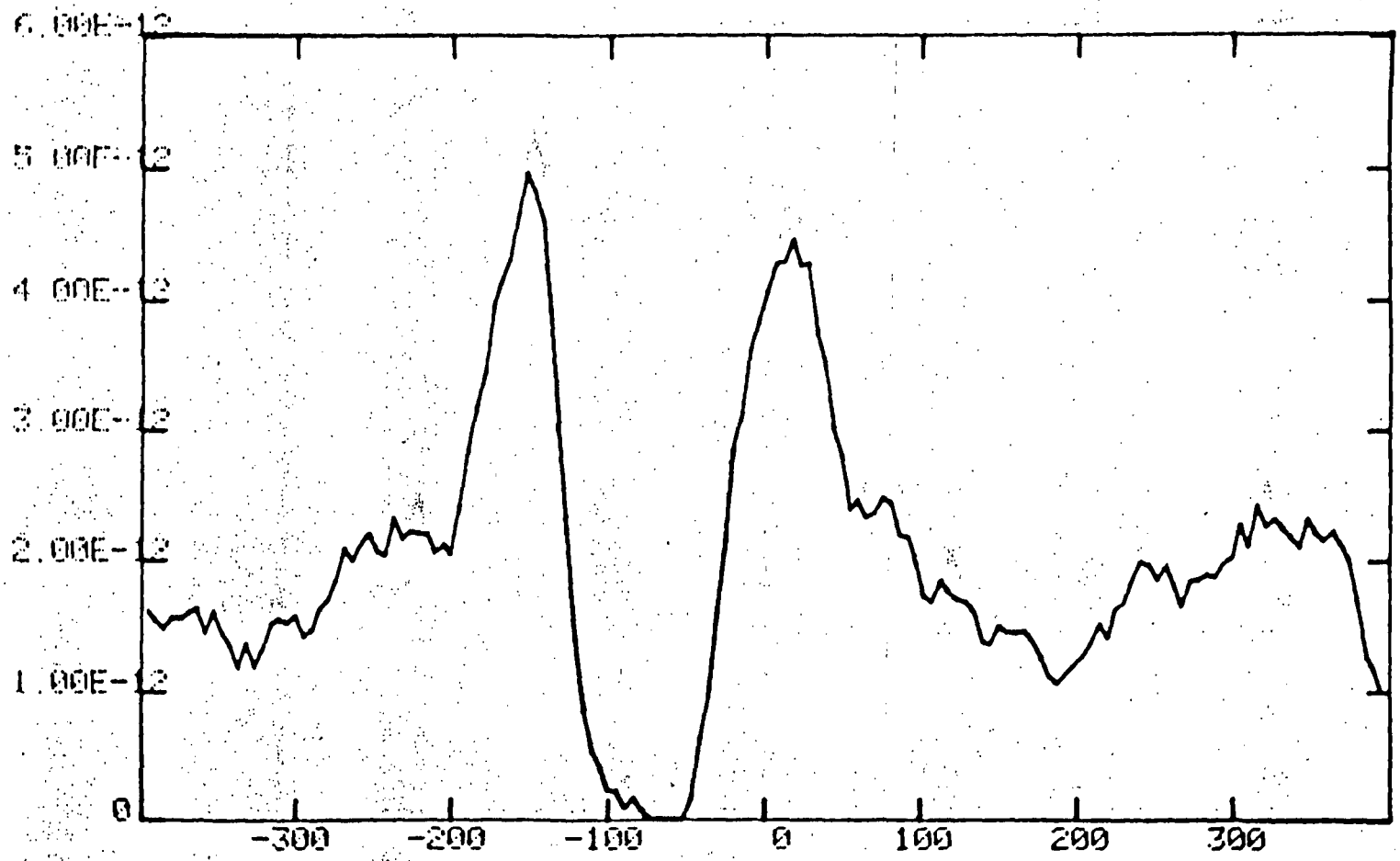

FIG. 6

§ Per SWP 3031

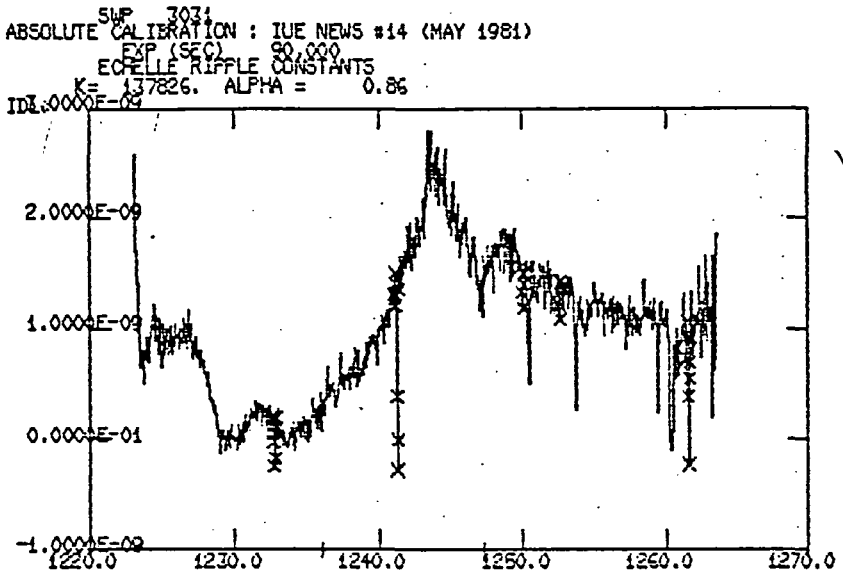

193

NV

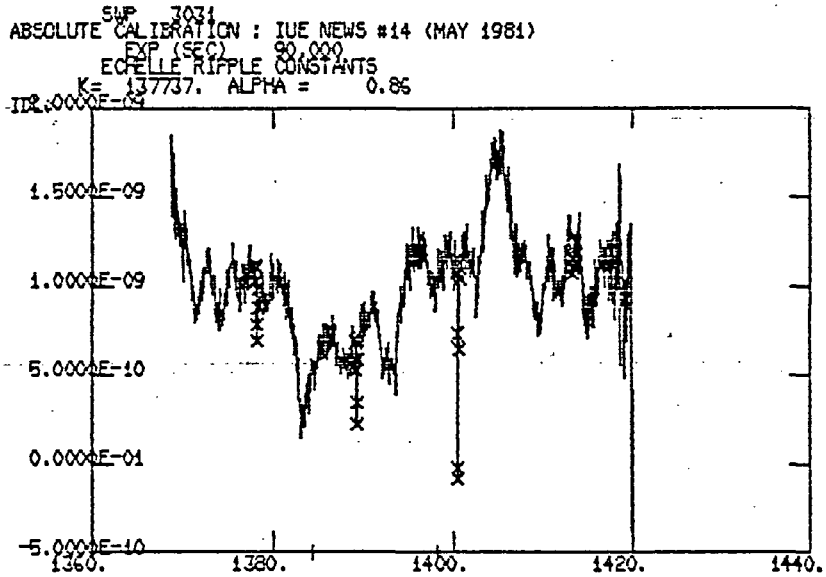

194

SiIV

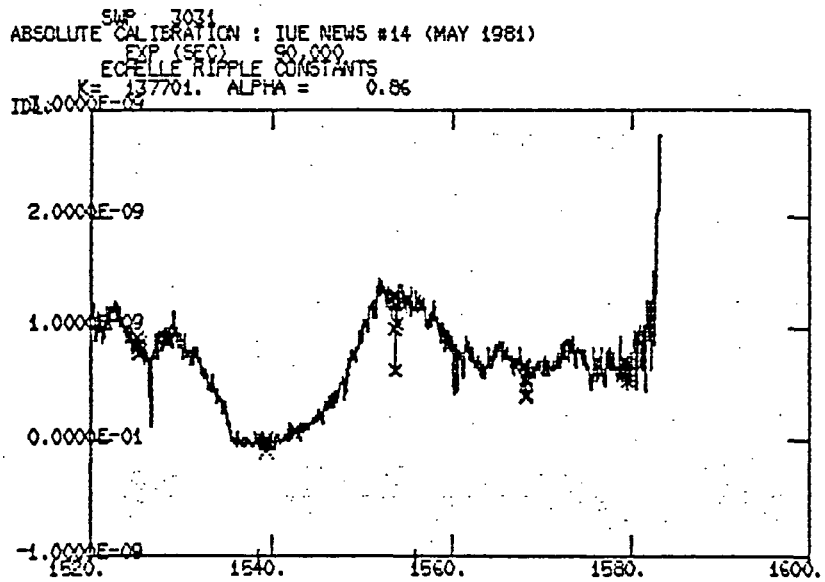

195

CIV

FIG. 7

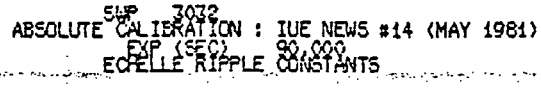

Rho Leo

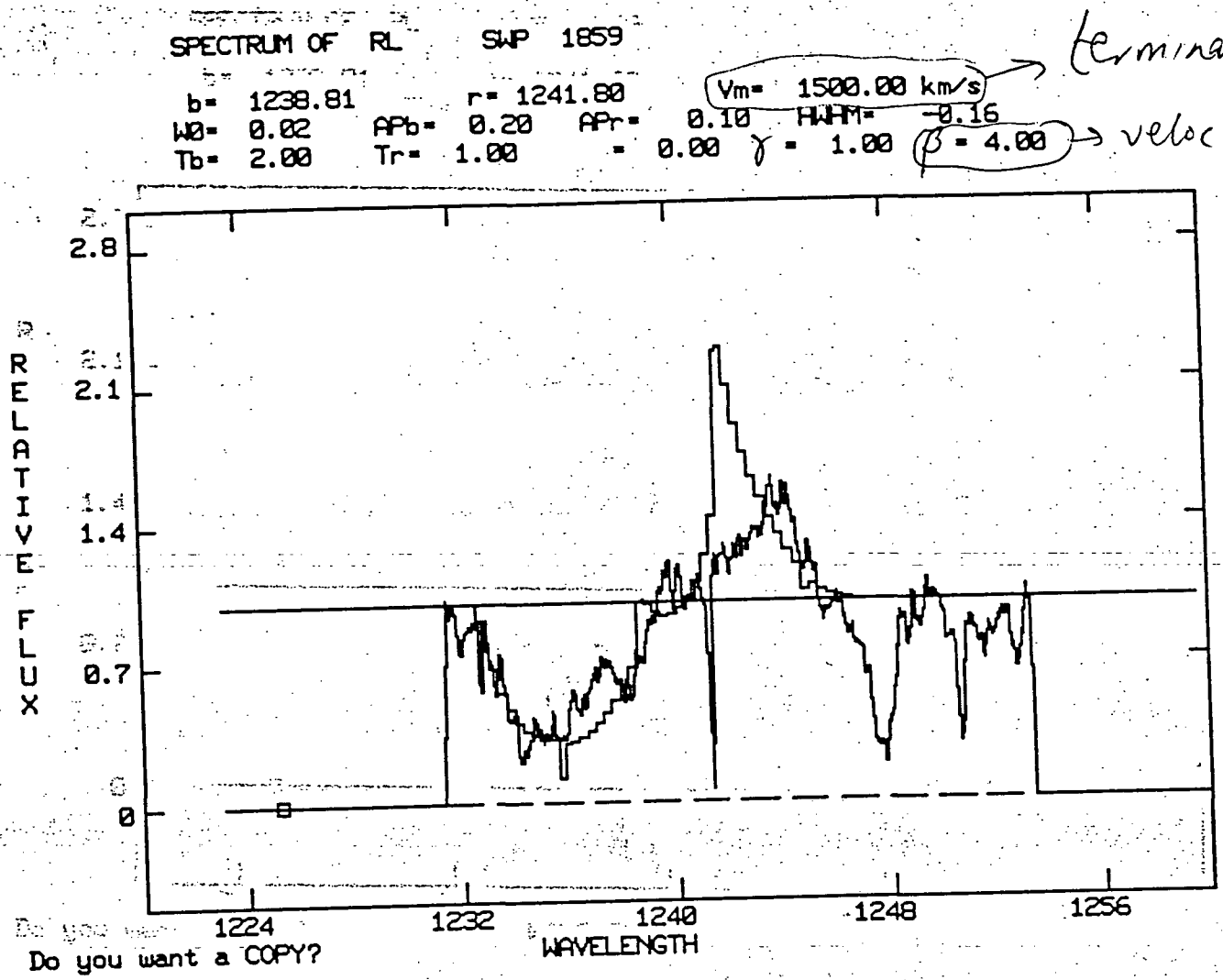

histogram = theoretical P Cyg profile
continuous line = data

FIG. 8

R Ho Leo

SPECTRUM OF RL SWP 1859

b= 1548.19 r= 1550.76 Vm= 1500.00 km/s
W0= 0.02 APb= 0.60 APr= 0.30 HWHM= -0.13
Tb= 12.00 Tr= 6.00 [illegible] = 0.00 [illegible] = 2.00 [illegible] = 4.00

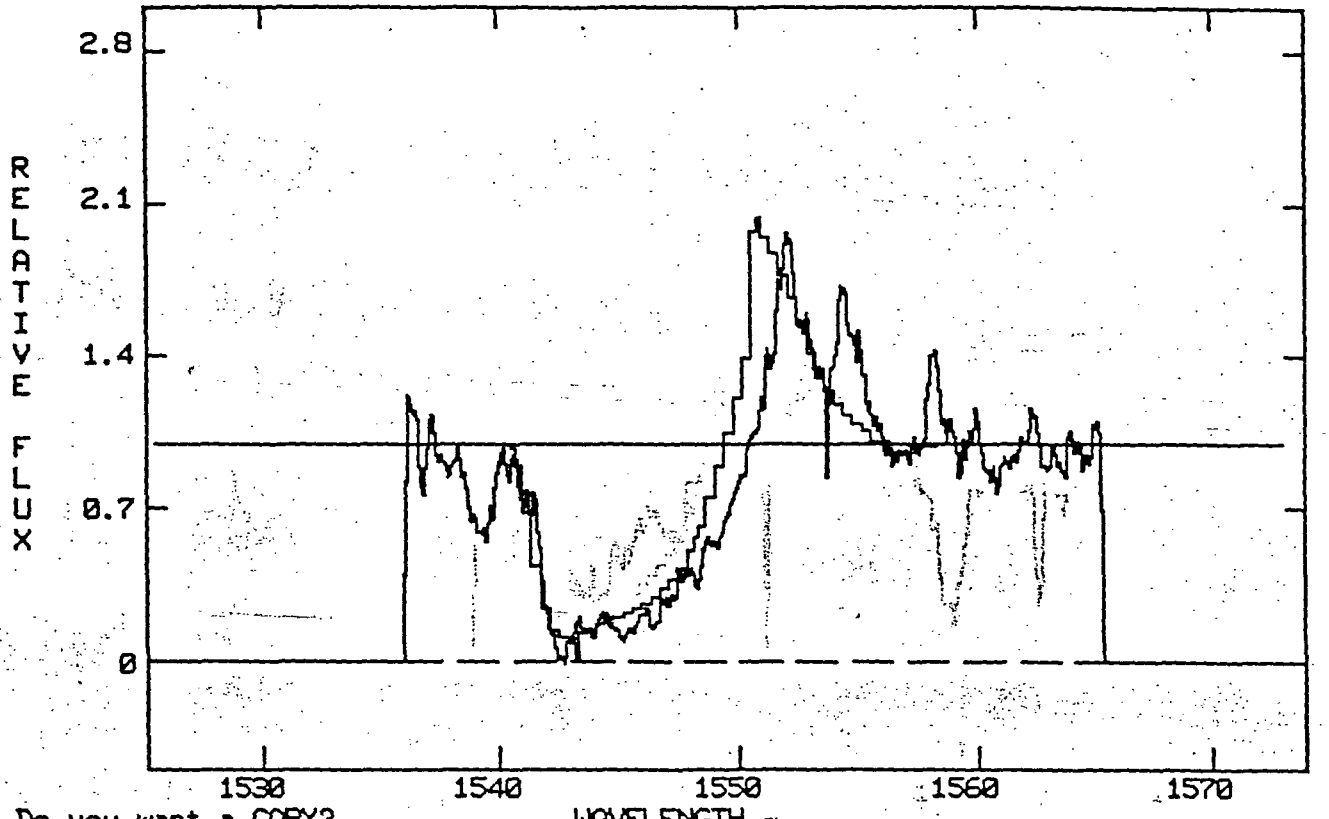

Do you want a COPY?

C IV line

Fig. 9

Rho Leo

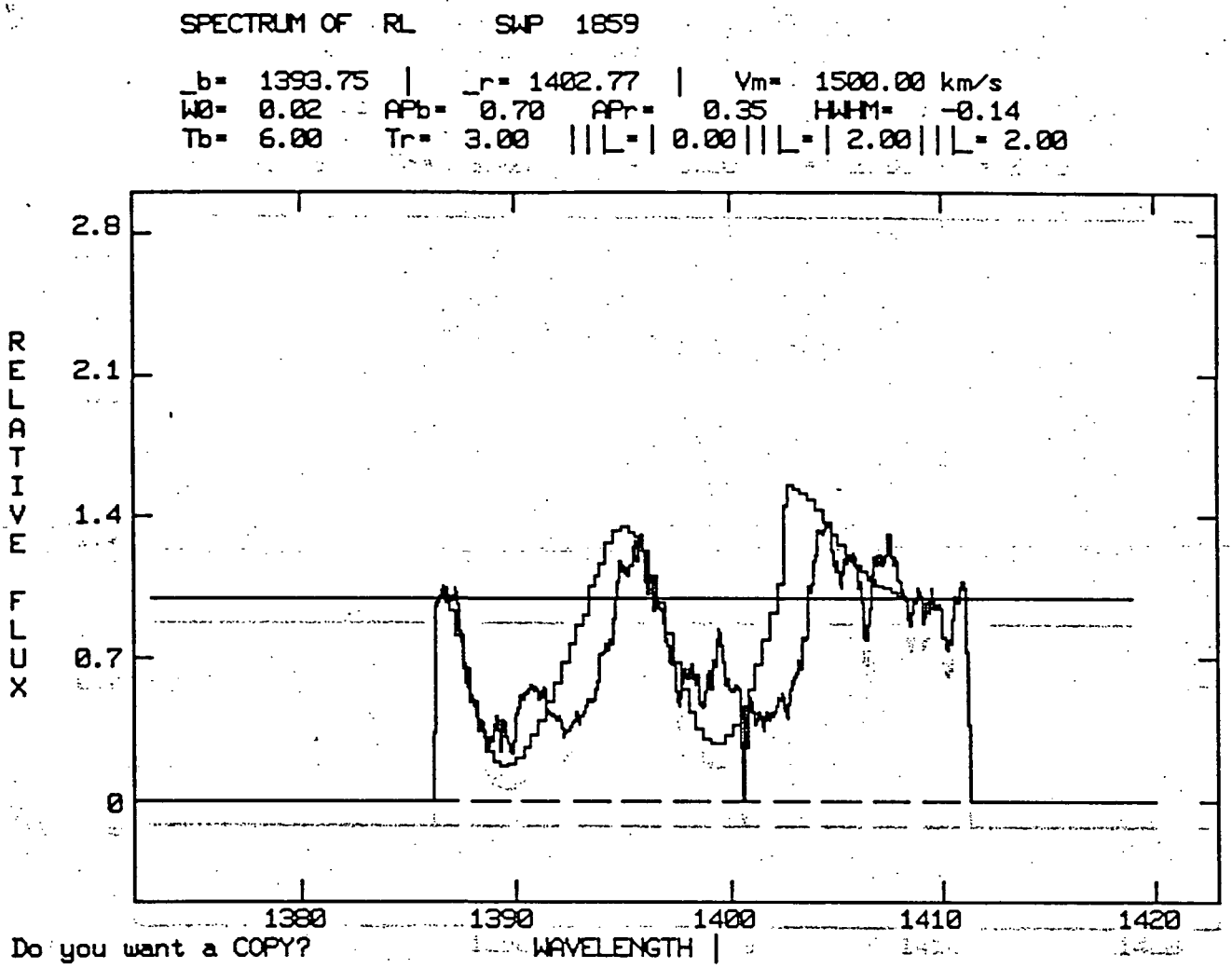

Si IV doublet

Fig. 10

χ i Persei

photospheric abs. central depth

SPECTRUM OF SWP 3035

b= 1548.19 r= 1550.76 Vm= 3800.00 km/s terminal velo
W0= 0.02 APb= 0.90 APr= 0.45 HWHM= 0.10
Tb= 16.00 Tr= 8.00 = 0.00 γ= 4.00 β= 4.00

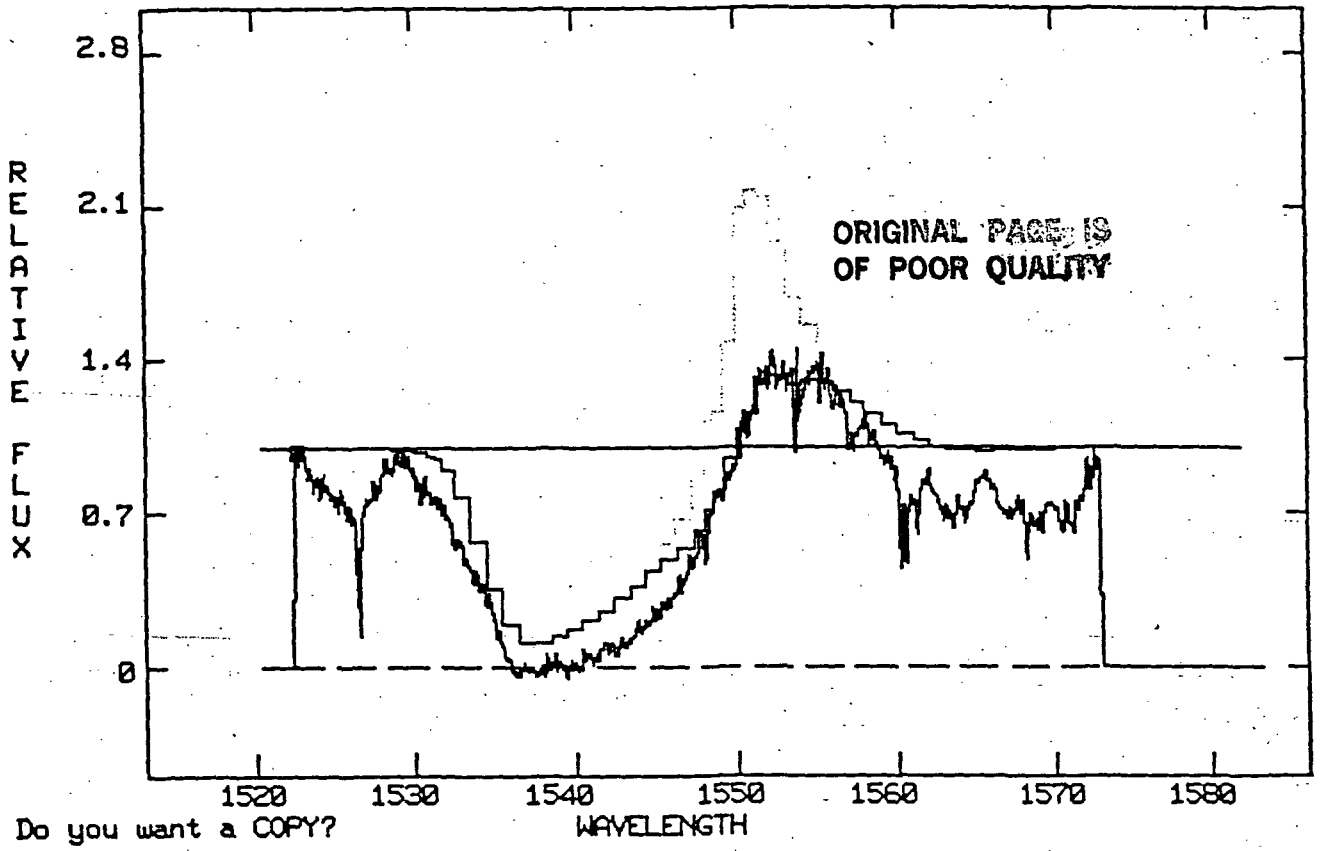

worst photo line
0.90 0.45
2 Å HWHM

FIG. 11

DELTA ORI

SPECTRUM OF DO SWP 4018

b= 1548.19 r= 1550.76 Vm= 2600.00 km/s
W0= 0.02 APb= 0.80 APr= 0.40 HWHM= -0.15
Tb= 8.00 Tr= 4.00 = 0.00 γ = 2.00 β = 2.00

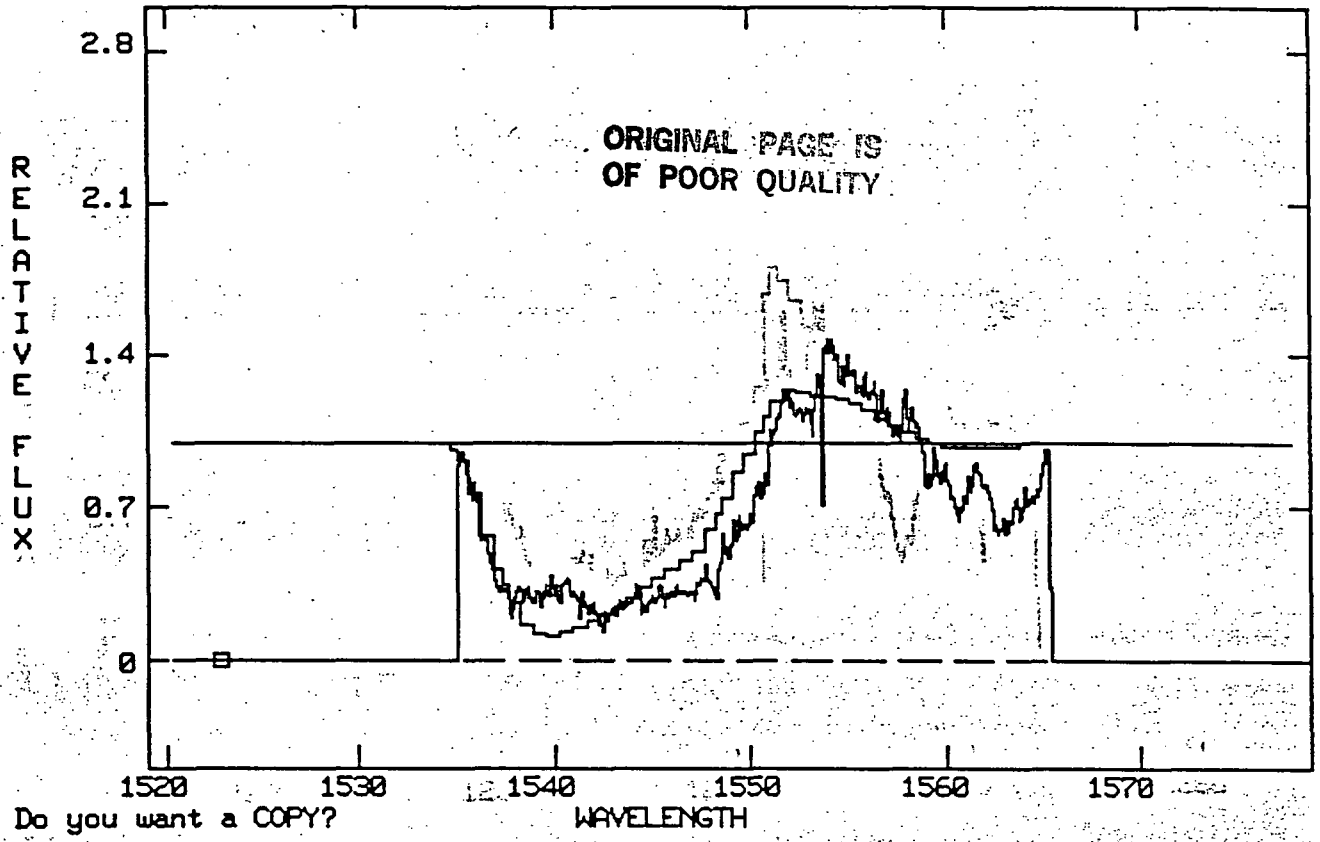

Do you want a COPY?

C IV line

FIG. 12

DELTA ORI

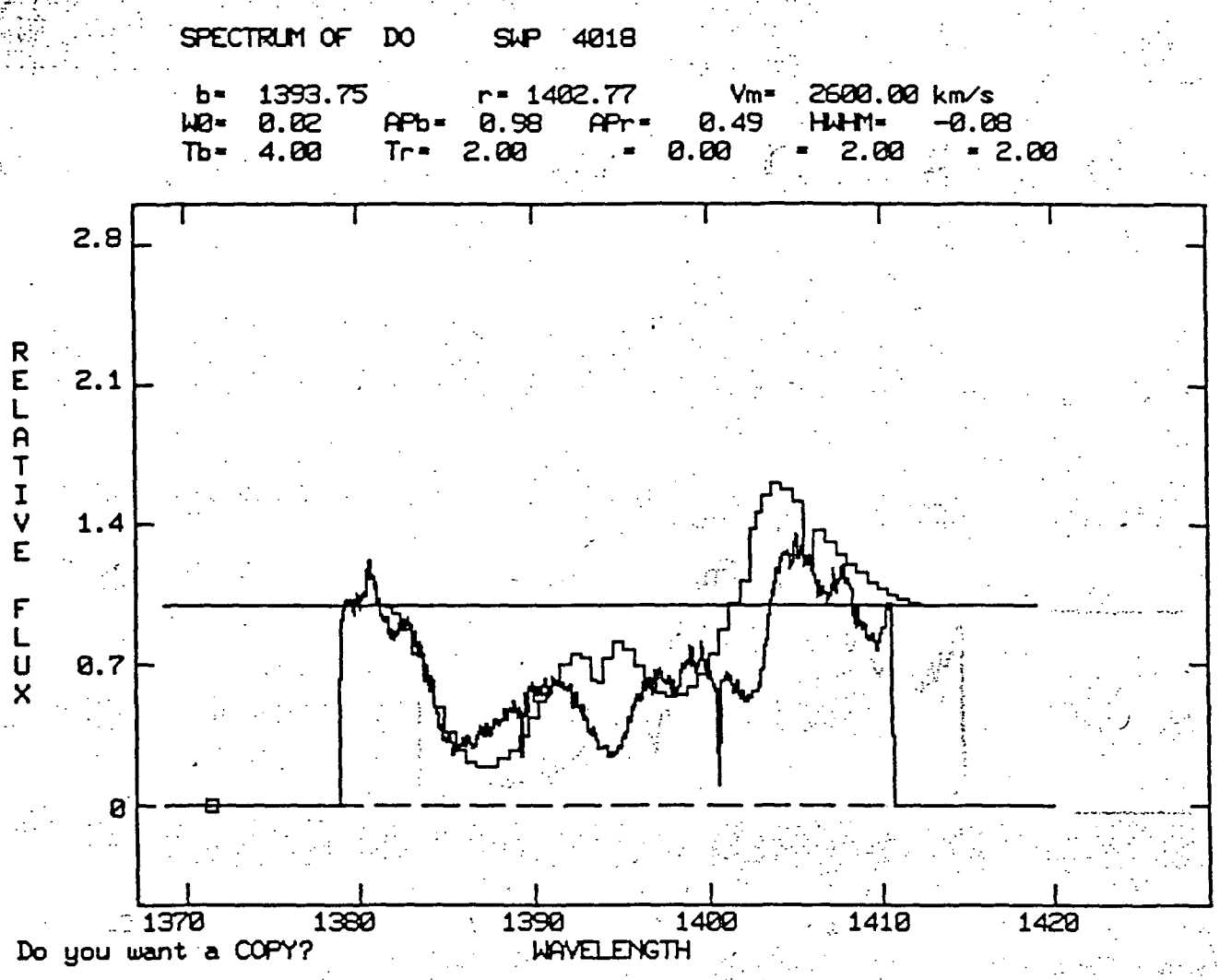

Si IV line

Fig 13

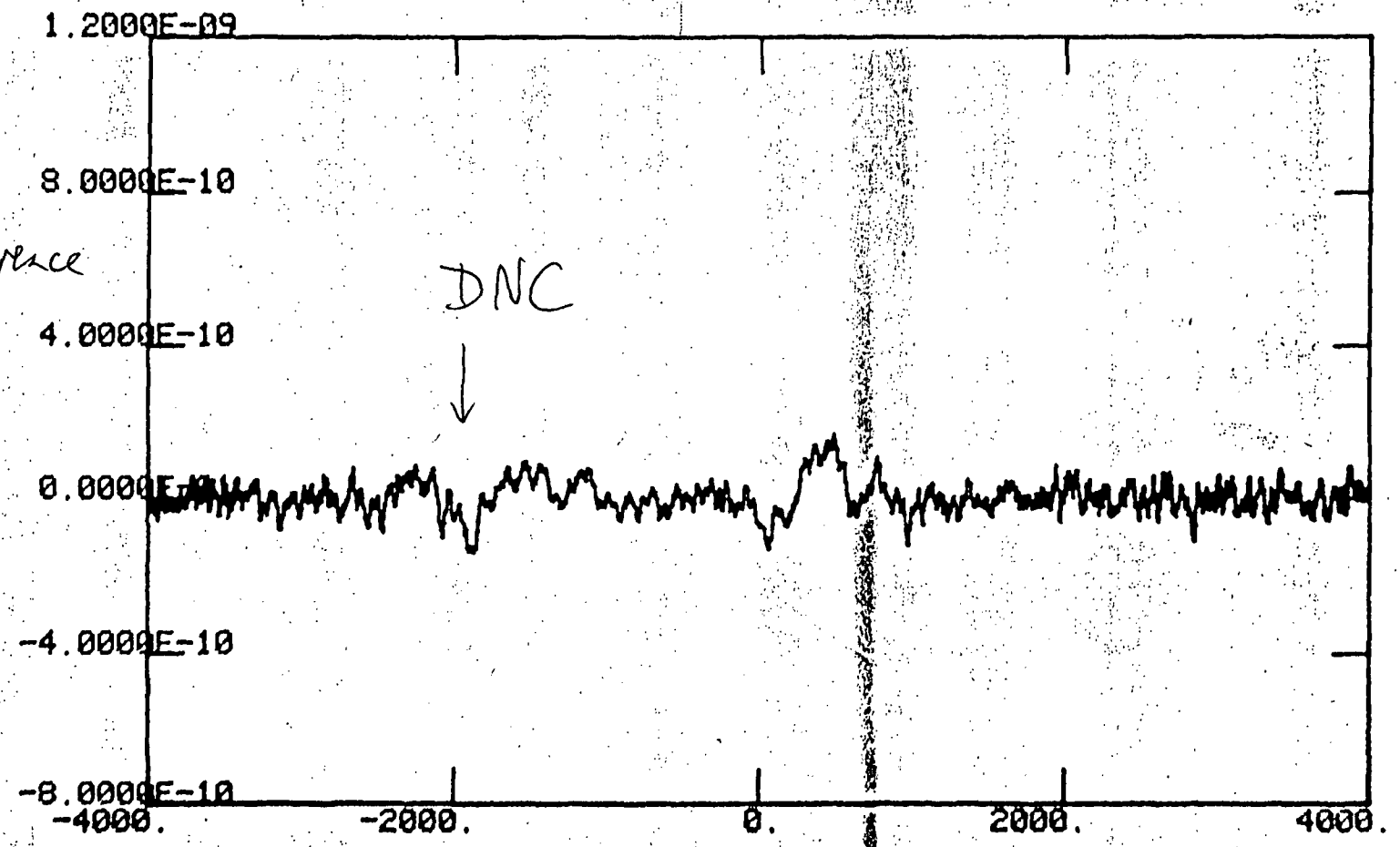

Flux difference

SWP 21003
−SWP 21051

FIG. 14

Astron. Astrophys. 881, ▮▮▮–▮▮▮ (1986) 07(19.32.1; 19.48.1; 19.09.1; 19.25.1; 12.03.1)

ASTRONOMY AND ASTROPHYSICS

Displaced narrow absorption components in the spectra of mass-losing OB stars: Indications of corotating interaction regions?

D.J. Mullan[1,2]

[1] Dunsink Observatory, Dublin 15, Ireland
[2] Bartol Research Foundation, University of Delaware, Newark, DE 19716, USA

Received October 22, 1985; accepted March 10, 1986

Summary. Narrow absorption components have been detected in recent years in the UV spectra of many OB stars. These narrow components exhibit large displacements to negative velocities. Here we point out that many of the properties of these components appear to be understandable in terms of co-rotating interaction regions (CIRs) in stellar winds. However, certain features of the CIR scenario cannot yet be tested by available data.

Key words. early-type stars – mass loss – ultraviolet spectra

1. Introduction

The most characteristic signature of stellar mass loss in OB stars is the presence of the so-called P Cygni line profiles in the spectrum. These consist of a redward emission peak plus a broad blueward absorption trough, extending to a more or less sharply defined edge at the "terminal velocity", v_t. The P Cygni profiles typically occur in the resonance lines of abundant ions: in OB stars, for example, they have been observed in the resonance lines of C IV, Si IV, and N V. (For a systematic graphical presentation of how the P Cygni profiles behave in OB stars of various luminosities, see Snow and Morton, 1976 and Walborn and Panek, 1984.) P Cygni profile have been modelled extensively in terms of a spherically symmetric wind (e.g. Gathier et al., 1981; Garmany et al., 1981; Garmany and Conti, 1984).

Recent data, however, have uncovered a further spectroscopic signature of mass-losing stars: narrow absorption components which are usually displaced to large negative velocities. (Only one case of a red shift is known to the author (Bruhweiler, 1985): in all other cases the shifts are to the blue.) These displaced narrow components (DNCs) can occur either as features superposed on a background P Cygni profile, or, in the absence of a P Cygni profile, simply as transient discrete absorption features in the continuum. (The latter case occurs in some Be stars: cf. Barker and Marlborough, 1985). Snow (1977) undertook a systematic observational program on DNCs, and a systematic study of DNCs based on data from the Copernicus satellite is contained in the paper by Lamers et al. (1983; hereafter LGS). Data from the IUE satellite have been used by Henrichs (1984; hereafter H84) to review DNC properties. Very recently, Prinja and Howarth (1985; hereafter PH) have reported extensive modelling of DNC in IUE data of 22 OB supergiants and giants. For a broad ranging discussion of DNCs, see the comments of many participants at the first Trieste workshop (Stalio, 1982).

The discovery of DNCs in an increasingly large number of stars of various spectral types suggests that an explanation of these features may contribute significantly to our understanding of winds from stars of all types. In Sect. 2, we summarize the reported properties of DNCs with a view to evaluating one particular scenario for DNC formation: the scenario which we wish to evaluate involves corotating interaction regions (CIRs) in the stellar wind. CIRs have been proposed recently (Mullan, 1984a, b) as a possible explanation for four apparently unconnected types of phenomena: X-ray emission from stellar winds, "warm" gas in the winds of so-called "hybrid" stars, "chromospheric" gas in the winds of red supergiants, and discrepant asymmetries in the resonant emission lines of Mg II and Ca II in cool giants. In Sect. 3, we summarize the relevant features of the CIR scenario. In Sect. 4 we discuss the extent to which DNC properties support the CIR scenario, and we also point out the limitations of the scenario.

2. Displaced narrow components (DNCs)

In the spectrum of an OB star, DNCs appear as transient aborption features shifted to the blue of the photospheric line center. Once a feature appears, it tends to remain fixed in velocity during its lifetime. (However, as an exception to this statement, Henrichs et al. [1980] have reported a DNC which does not remain constant in time.) In many stars, DNCs seem to "prefer" a certain velocity: a new DNC may appear at the same velocity where an earlier DNC had been observed. During the lifetime of a DNC, the absorption strength may vary at the tens of percent level, on time scales which in different stars range from hours to days. Most DNCs decay to undetectable levels on similar time-scales. During the decay, the velocity remains constant ("decaying in place"). Lifetimes of some DNCs appear to be much longer than the time-scales mentioned above: in the case of the dwarf star Zeta Ophiuchi, a DNC has been reported to persist for at least 10 years at a particular velocity. The observations of Zeta Oph have not been continuous, and so one cannot say definitely that a single DNC has persisted: this star, in fact, is known to be a non-radial pulsator, and mode switching in such a star is associated with outbursts of energy in the atmosphere (as shown by

Send offprint request to: D.J. Mullan (American address)

episodes of H-alpha emission; Vogt and Penrod, 1983). Such outbursts probably also disturb the wind and the DNC. Another example of a long-lived DNC is provided by P Cygni (Lamers et al., 1985): here, the DNC persists for $\gtrsim 5$ years, and is certainly one and the same DNC during that interval.

Velocity centroids of DNCs are found to be in general closer to v_t than to zero: centroids are observed at typically $(0.5 - 0.9)v_t$. PH note three exceptions to this rule, with DNCs in three stars centered at velocities of 0.19, 0.37, and 0.46 v_t. PH noted that these three stars had unusually large values of the ratio v_{eq}/v_t (where v_{eq} is the equatorial rotation velocity). (We will return to these three fast rotators below.) However, even including the three exceptional cases, it is important to note that DNC have generally not been detected at velocities close to zero. Since stellar wind velocity is expected in general to increase with increasing radial distance from the star, the lack of DNCs at low velocities is most readily interpreted as evidence for the absence of the entity which causes DNCs in the inner wind. (PH explain the lack of DNC at low velocities as being due to fast variations in the inner wind, and wide profiles there.) If one were to suggest that the entity which causes DNCs is something ejected from the star directly, then it would appear to be difficult to account for the fact that no observation has yet "caught" the ejection close to the star. One possible example of having "caught" such a DNC in α Crucis (BIV) is reported by Gry et al. (1984): the DNC lies at low velocity ($\lesssim 0.1\ v_t$), and varies on a time-scale of order one hour.

The widths of DNCs in velocity are found to be small compared with the centroid velocity: widths are typically $(0.01 - 0.1)\ v_t$. The small widths are striking, especially in view of the observation that the features persist for fours or days at a fixed velocity centroid. Whatever the origin of DNCs, they are apparently capable of maintaining a well defined narrow range of velocities in the stellar wind. If the wind velocity is a monotonic function of radial position, the narrow widths and constant centroids of DNCs imply that the features which create DNCs are confined to a well-defined range of radial distances from the star. In the case of the 3 fast rotating stars reported by PH as having slower DNCs than typical, the velocity widths are also atypically large, up to 0.21 v_t.

When DNCs are observed in the spectrum of a star in lines of several different species, the central velocities are identical (within the measurement errors) in all species regardless of ionization potential (PH). However, the strengths of DNC are not equal in different species: there is a tendency for the lines to be stronger in ions of anomalously high ionization (e.g. OVI; cf. GLS). Whether this means that the DNC are formed in gas of systematically higher temperature is not clear: PH have found that as far as the dominant stages of ionization are concerned, it is not always obvious whether or not the DNC have higher ionization than the underlying P Cygni profile.

The column densities, CD, in the DNCs have been derived by PH for a sample of 22 OB stars: the values range from $\log CD = 13.6$ to 15.0 (in units of cm^{-2}). The average column densities in lines of N v, C iv, and Si iv are $3.9\ 10^{14}$, $4.2\ 10^{14}$, and $2.5\ 10^{14}\ cm^{-2}$. The small dispersion in these values among the various stars in the sample is noteworthy.

Multiple DNC are observed in certain stars at some epochs e.g. P Cygni (Lamers et al., 1985), ζ^{-1} Sco (Burki et al., 1982). The record is held by a subdwarf (HD 12822 OB) where as many as 10 different DNCs may coexist (PH). Others stars have not yet been observed to show more than a single DNC. However, PH have stressed the ubiquity of DNC in the sample of stars which they studied (22 stars with special types O4-B1, luminosity classes V, III, and I): "Every star with reasonably unsaturated lines has shown evidence for (DNC) at some time". In a broader survey, H84 examined spectra of 146 stars of spectral types O3 – B8, and found that among the supergiants ($M_{bol} < -7.5^m$), more than 50 percent showed DNC. However, among the less luminous stars, the only stars to show DNC were Be stars (10 out of a sample of 30 showed DNC) and O subdwarfs (2 out of a sample of 4).

The Be stars are of particular interest in the study of DNC because the underlying P Cygni profile disappears at times, leaving only the DNC in the spectra (Barker and Marlborough, 1985). And the DNC themselves may disappear and reappear in time, with or without an underlying P Cygni absorption trough. In the Be stars also, the range of DNC velocities relative to the wind terminal speed is larger, not necessarily confined to the higher velocities. In some cases, it appears that the entire absorption trough may be of a number of separate (but overlapping) DNCs. The persistence of particular DNCs at a fixed velocity during their lifetime has also been pointed out in the Be stars by Barker and Marlborough. The time scales for decay of the column density of DNCs in Be stars is found to be again on the order of a few days. Barker and Marlborough point out that in some of their stars, there seems to be no C iv absorption close to zero velocity, as if the onset of C iv formation is "postponed" until the wind reaches a certain distance from the photosphere. The DNC profiles in Be stars are observed to have abrupt longward edges and extended shortward winds, i.e. similar to the standard absorption trough shape of the entire wind profile. This leads Barker and Marlborough to the conclusion that in Be stars, the winds may be discontinuous or patchy entities: "Embedded within the wind there must be localized regions, which either release material into the wind some distance above the photosphere ... or which abruptly trigger superionization of the ambient wind at specific radial distance". For further discussion of DNC's in a particular Be star, see the extensive recent study by Grady et al. (1985).

The discussion of how DNCs are related to the underlying P Cygni profile in Be stars suggests that we should examine the same question in other OB stars. The situation is not yet clear. For example, in a pair of spectra of ξ Persei, the P Cygni profile at low velocities was observed to weaken between the two exposures, while a DNC at faster velocities became strengthened (H84). This suggests that some of the "underlying" wind material may have been "swept up" into the DNC. If the underlying P Cygni trough is indeed a superposition of multiple DNCs, then as the DNCs vary in intensity, the terminal velocity of the trough should also vary by typically the width of a DNC. In fact, PH report on some of their stars having changes in v_t by $100 - 300\ km\ s^{-1}$: this would be consistent with typical widths of DNC. However, the other stars in their sample do not yet show this effect.

Perhaps we should not expect that features of Be stars should be reproduced exactly in other classes of stars. A special characteristic of Be stars, for example, is their fast rotation. There is some indication that in fact DNCs are more likely to form if the rotation is fast. (The importance of fast rotation has already been noted above in discussing OB stars which show DNC at "low" velocities.) Thus, H84 examined a sample of 30 Be stars with a

distribution of $v \sin i$ values peaking in the range $v \sin i = 200 - 250\,\mathrm{km\,s^{-1}}$. The distribution of $v \sin i$ values outside the peak region was rather symmetric: 33 percent had $v \sin i$ values less than $200\,\mathrm{km\,s^{-1}}$, while 33 percent of the stars had $v \sin i$ larger than $250\,\mathrm{km\,s^{-1}}$. However, among the 10 stars which showed DNC, this symmetry disappeared. Thus, although the peak in their $v \sin i$ distribution also occurred in the range $200 - 250\,\mathrm{km\,s^{-1}}$, only 10 percent of the stars lay on the low side of the peak (i.e. had $v \sin i$ less than $200\,\mathrm{km\,s^{-1}}$), while 40 percent of the stars lay on the high side of the peak (i.e. had $v \sin i$ larger than 250 km sec^{-1}). Thus, the distribution of $v \sin i$ values for the stars with DNC was certainly skewed towards higher values of $v \sin i$ to a much greater extent than the general sample of Be stars. Of course the statistics are too small to make this conclusion rigorous, but it is worth noting.

The importance of rotation in understanding the origin of DNC in OB stars has been stressed by PH. In particular, as we have mentioned, PH found that the three stars with the lowest velocity DNC's (in terms of terminal velocity) had the highest values for the ratio of rotational velocity to terminal speed.

3. Co-rotating interaction regions (CIRs)

Here, we summarize briefly the discussion of Mullan (1984a). No star is expected to emit its wind in a manner which is precisely circularly symmetric with respect to the rotation axis. (For a particular example of this in hot stars, see Pecker, 1982). Hence, as a result of the rotation, fast wind emitted along a certain radial vector will eventually overtake slower wind emitted previously by a different part of the star along the same vector. When the overtaking process occurs, the fast and slow streams adjust to each other's velocities in an interaction region. The interaction begins at the contact discontinuity between the streams, and it spreads out spatially in both directions as time progresses. If the velocity differential between fast and slow streams is large enough (greater than the local sound speed), the interaction region is bounded by a forward shock (moving out into the slow stream) and a reverse shock (facing towards the fast stream). Between the shocks, the velocity has a plateau. In a frame of reference fixed in space, the interaction region rotates with the angular velocity of the central star. Hence the name, Co-rotating Interaction Region. In a frame of reference which rotates with the star, the CIR appears as a spiral structure which begins at a definite radial distance, and expands in thickness as the wind flow carries the interaction to further distances.

In the solar wind, the radial thickness of the CIR as seen in the rotating frame is typically 10% of its radial distance from the sun. We shall use this property below in estimating typical column densities in CIRs in a stellar wind. In the solar wind, modelling of CIRs indicates that the velocity of the plateau in velocity remains essentially unchanged (at the level of a few percent) as the CIR propagates into the distant wind (Holzer, 1979).

The velocity plateau in a CIR in a stellar wind will be the most readily observable feature of the CIR if our line of sight happens to pass through the CIR. The signature of a plateau will be a narrow absorption feature in the spectrum. This is the main reason for examining the possibility that DNCs are associated with CIRs in stellar winds.

It is essential to note that a CIR does not form immediately at the surface of a star. A finite time is required for the fast stream to overtake the slow stream, and hence, the CIR always forms at a finite distance R_t from the star. With certain simplifying assumptions (Mullan, 1984a) it can be shown that R_t is proportional to the ratio of wind speed to rotational speed. On the basis of the properties of CIRs in the solar wind, it appears that the constant of proportionality is on the order of one stellar radius. Thus, to a first approximation, we can adopt

$$R_t/R_* \approx v_t/v_{eq} \qquad (1)$$

where v_{eq} is the equatorial rotational velocity of the star of radius R_*.

In the case of the solar wind, v_t is about $400\,\mathrm{km\,s^{-1}}$, while v_{eq} is about $2\,\mathrm{km\,s^{-1}}$. Hence, in the solar wind, CIRs do not form until the fast stream has propagated to a radial distance of about 200 solar radii (corresponding roughly to the orbit of the Earth). At such large distances from the sun, the acceleration of the solar is essentially complete; if we could take advantage of a distant vantage point to view the sun through a CIR, the corresponding DNC would have a velocity centroid very close to v_t.

In the case of other stars, the ratio of v_t/v_{eq} may be much smaller than the solar value, allowing CIRs to form much closer to the star. For example, in the sample of 22 OB stars discussed by PH, v_t is of order $1000\,\mathrm{km\,s^{-1}}$, while v_{eq} is of order $100\,\mathrm{km\,s^{-1}}$. In such stars, the above expression indicates that a CIR will form at typically 10 stellar radii from the central star. (We will use this value below when we estimate column densities in CIRs in the stars belonging to the PH sample.) In extreme cases, the ratio of v_t/v_{eq} may be sufficiently small to allow CIR formation to occur even closer to the star, within a few radii of the surface. The closer to the star the CIR forms, the more likely it is that the acceleration of the wind will not yet be complete at the location where the CIR forms. Hence the velocity plateau is expected to lie at lower velocities in the case of stars with smaller values of v_t/v_{eq}. This is an important prediction of the CIR scenario to which we will return below.

If we were to model how the absorption feature associated with a CIR would appear in the spectrum of a star (i.e. derive a line profile for the associated DNC), we would need to know the density enhancements associated with the shocks which bound the CIR. This would require use to solve a complex initial boundary value problem. In the solar wind, certain cases of this problem have been treated in considerable detail (Pizzo, 1983), and structures of great complexity can exist in the distant solar wind if the Sun happens to emit several streams simultaneously. However, in stellar cases, information about initial and boundary values is in general lacking. For example, what is the velocity differential between streams and what is their longitudinal extent? For velocity differentials, we might use the extreme range of terminal velocities observed in a given star. Thus, PH suspect that in some of their stars, v_t varies from epoch to epoch by $100 - 300\,\mathrm{km\,s^{-1}}$. And in the case of a Herbig Ae star, v_t has been observed to vary by about 30%, from 395 to $515\,\mathrm{km\,s^{-1}}$ (Praderie et al., 1984). If these are valid estimates of the velocity differentials in the winds of these stars, they are comparable to, but somewhat smaller than, the observed differentials in the solar wind (where "fast" streams have velocities which are up to $300 - 500\,\mathrm{km\,s^{-1}}$ faster than the slow wind). Until more detailed information becomes available on the initial/boundary conditions in stellar winds, the evaluation of DNC properties corresponding to a CIR must remain approximate. Those properties which can

be evaluated are found to be consistent with a number of different data sets (Mullan 1984a, b).

In a systematic study, Prinja and Howarth (1984) have modelled the DNC which appears in a P Cygni profile if a velocity plateau is inserted in the wind. In that work, no physical origin was discussed for the plateau. Now that CIRs are seen to serve as a possible cause of a plateau, the work of Prinja and Howarth (1984) may serve as a useful indicator of the spectral signatures of CIRs which form at certain radial distances in a stellar wind.

4. Can CIRs account for DNCs?

4.1. Strengths of the CIR scenario

(a) Multiple DNCs can be understood in terms of emission of several streams from a star: this would yield multiple CIRs in the wind at any moment, depending on the time history of the various streams.

(b) The narrowness of DNC can be attributed to the flatness of the velocity plateau within the CIR.

(c) The displacement of DNC from zero velocity can be attributed to the finite radial distance from the star at which CIR's form in a stellar wind.

(d) Decays of DNC "in place" (i.e. at essentially constant velocity) can be attributed to propagation of the line of sight through a CIR through the distance wind. In such cases, the acceleration of the wind is complete, and the mean velocity of the CIR plateau remains very nearly constant as the line of sight through a CIR propagates to infinity (cf. Holzer, 1979). The velocity at which the DNC "sits" is the CIR plateau velocity i.e. intermediate between the velocities of the fast and slow streams (v_f, v_s). Hence if we identify v_t with the fast stream $v_t = v_f$, the DNC will "sit" at a velocity v(DNC) such that $v_s < v(\mathrm{DNC}) < v_f = v_t$. Thus, along a particular line of sight, v_f determines v_t, but v(DNC) is determined by $\sim 0.5\,(v_s + v_f)$.

(e) Time scales for decay of DNC's would be determined by wind speed and by the distance to which the line of sight through a CIR would have to be carried in order to make the optical depth of the plateau material fall below detectability. For example, consider stars with $R_* = (10 - 100)\,R_{(\mathrm{sun})}$, $v_t = (1000 - 3000)\,\mathrm{km\,s^{-1}}$, and $v_{eq} = 50 - 200\,\mathrm{km\,s^{-1}}$. In such stars, CIRs will form at R_t roughly $(5 - 60)\,R_*$, i.e. at distances of order $(0.4 - 40)\,10^{13}$ cm. The wind density falls off by a factor of 4 between R_t and $2R_t$, but the thickness of the CIR also expands by roughly a factor of 2 (cf. Mullan, 1984a). Hence, the optical depth of the DNC will decay by a factor of about 2 on time scales which may be as short as $\lesssim 1$ day, or as long as ~ 50 days. Such time scales are consistent with the results of PH.

(f) Stars with highest ratios of v_{eq}/v_t are expected to form CIRs (and therefore DNCs) at the smallest velocities (expressed as fractions of v_t). This is consistent with the findings of PH.

(g) Local heating of the wind in the forward and reverse shocks of the CIR can explain why the level of ionization is higher in the DNCs than in the background wind. The amount of local heating is sensitive to the local jump in wind velocity across the shock. In a purely gasdynamic shock, a jump in velocity by $100\,\mathrm{km\,s^{-1}}$, for example, heats gas to temperatures of order 10^5 Kelvin: these are precisely the order of magnitude of the temperatures which would be required to explain the presence of spectral lines of the best known "superionized species" (C IV, Si IV, N V, and O VI).

(h) The evolution of the interaction as a fast stream overtakes a slow stream would have the effect that previously slow material would be swept up from low velocities into a DNC. This could explain an example quoted by H84 (in the spectrum of ξ Persei) in which a range of (low) velocities in the background P Cygni profile was observed to weaken as a DNC at higher velocity built up in strength.

(i) Departure from spherical symmetry is an essential aspect of the CIR scenario. This also may contribute to making it difficult to "catch" the formation of DNC at low velocities, i.e. close to the star.

(j) The fact that the CIR creates a physically identificable structure in the wind where all species pass through a plateau in their velocity, explains why the velocities of DNCs are identical in all ion species.

(k) Quantitatively, the column densities in the DNCs which were studied by PH can be reproduced satisfactorily in the context of the CIR scenario provided that the fractional abundances of the ions C IV, Si IV, and N V are some tens of percent. To see this, note that the (hydrogen) column density in a single radial pass through a CIR located at $10\,R_*$, with thickness R_*, is

$$CD(\mathrm{H}) \approx 0.01\,n_0 R_* \approx 0.01\,\dot{M}/(4\pi v_t R_* m_H) \qquad (2)$$

Here, n_0 is the density at the base of the wind, $\dot{M}$ is the mass loss rate, and m_H is the mass of the hydrogen atom. PH provide data on $\dot{M}$, v_t and R_* for each of 22 stars. Using these, we find that CD(H) for all of the stars in their sample lie within a factor of 2 of the mean value

$$CD(\mathrm{H}) \approx 10^{19}\,\mathrm{cm^{-2}}. \qquad (3)$$

Applying the usual cosmic abundances, we then find column densities for the elements C, N, and Si for a single radial pass through a CIR to be $3\,10^{15}$, 10^{15}, and $3\,10^{14}\,\mathrm{cm^{-2}}$, respectively. Comparing these with the mean CD values derived by PH for the ions C IV, N V, and Si IV in the DNCs in their sample, we find that the CIR can reproduce the observed CD if the fractional abundances of C IV, N V, and Si IV are about 10%, 40% and 80% respectively. Such abundances are plausible if the temperature of the CIR material is of order 10^5 K. (Temperatures in DNCs must be about this value; otherwise, lines of C IV, Si IV, and N V would not be detectable.)

(l) Lamers (private communication) has pointed out the eq. (2) can be cast in the form

$$CD(\mathrm{H}) \sim R_t^{-2} f R_t \sim R_t^{-1} \qquad (4)$$

where fR_t is the thickness of the CIR. Thus, in any one star, CD(H) is predicted to decrease as R_t increases. However, increasing R_t is associated with increasing v(DNC). Hence, we expect that CD(H) will decrease with increasing v(DNC) in any one star. Hesrichs (H84) has in fact reported such a relationship in several stars.

(m) In certain stars, it is remarkable that DNCs "prefer" a certain velocity. This implies that rather stable velocity structures persist in the atmosphere. One such structure immediately suggests itself by analogy with the solar corona: Open field regions favour fast wind, while closed fields favour slower wind. Consider then the case of a star where the global field is a dipole. In a gross sense, such a star would act as a source of basically two streams at all times, one from the polar caps, the other from the magnetic equator. In general, the magnetic axis does not coincide with the

rotation axis (hence the nomenclature, "oblique rotator"). As a result, fast wind will have the opportunity to interact with slow wind. In such a case, the DNC would lie at a preferred velocity immediate between the velocities of the polar and equatorial winds. To the extent that the basic two-component wind is valid for oblique rotators, one would expect to find only one DNC in such stars. (Multiple DNCs would require a multi-component wind.) And as long as the magnetic properties remain invariant, the "preferred" DNC velocity would remain constant.

(n) The CIR scenario predicts that DNCs should appear only as blue-shifted features in the spectrum of a single mass-losing star. However, in a binary, if the mass-losing star is in a geometrically suitable position, red-shifted DNCs may be detectable in the spectrum of the companion. The only case so far reported of a red-shifted DNC (Bruhweiler, 1985) occurs in the spectrum of a hot star in a binary with a cool giant (the latter presumably a mass-loser). It is a prediction of the CIR scenario that the red-shifted DNCs should disappear when the mass-loser is more remote from the Earth than the hot star.

4.2. Limitations on CIR scenario

(a) No dynamical calculations yet exist to evaluate how flat the velocity plateau in a stellar CIR might be. It may be that extreme flatness occurs only in highly supersonic flows in wind regions where acceleration is essentially complete (such as those modelled by Pizzo (1983) in the solar wind). The results of PH suggest that when DNCs form at lower velocities, the DNCs are also wider; this would be consistent with less flat plateaus if the CIR forms in the accelerating region of a wind, but more data are needed to establish whether or not a correlation exists between DNC widths (i.e. plateau "flatness") and DNC centroid velocity (i.e. plateau location) in each stellar wind.

(b) The velocity law $v(r)$ is not known in detail for any star (although certain laws are theoretically preferred in radiation driven winds). Hence, we cannot at present readily convert an observed DNC velocity to an interaction radius, R/R_*.

(c) We do not yet know if "decay in place" is a general property of stellar DNC. If a case could be established where the velocity of a particular DNC decreased as the DNC decayed, it might be difficult to interpret such behavior in terms of CIR outward propagation.

(d) If the decay time-scale of DNC depends on propagation through the wind, then DNCs at high velocities in the spectrum of a star should have a shorter lifetime than those at low velocities in the same star. This has not been confirmed or refuted for any star.

(e) Shock heating can be tested by seeking for a correlation between the velocity jump across the CIR (i.e. the velocity differential between fast and slow wind) and the amount of "superionization" in the DNC. No evidence for or against such a correlation yet exists.

(f) It is possible that variations which have been reported in v, from several stars as a function of time may be due to formation and disappearance of CIRs in the distant wind, where the plateau velocities would be difficult to distinguish from the terminal velocities. But higher spectral and time resolutions will be necessary before this can be established more firmly.

(g) It is not yet known how the amount of slow material which "disappears" from a background P Cygni profile compares with the amount of CIR material which "appears" in a DNC. Such a comparison would be an important check on the CIR scenario.

5. Conclusion

Archival IUE spectra have provided an extensive body of information on the properties of DNC (H84; PH). The data suggest that CIRs provide a useful working hypothesis for the interpretation of DNCs in stars of various types. CIRs were originally proposed as an explanation of excessive heating in the winds of stars of a broad range of spectral types. Now it appears that DNCs may also serve as a useful probe of CIR properties in winds of many stars. However, the discussion in the present paper suggests that before such a probe can be quantitatively successful, modelling of the stream-stream interactions in various classes of stellar winds must be undertaken. Such modelling in the solar wind has attained a considerable degree of sophistication in the last few years, but no work has yet been attempted in stellar winds.

It is anticipated that further examination of the extensive IUE archives, plus future planned observing schedules (particularly at specific time intervals to follow the evolution of a single DNC) will help to decide the extent to which the CIR scenario is a valid interpretation of DNCs.

Acknowledgements. I would like to thank Professor P.A. Wayman and the Dublin Institute for Advanced Studies for hospitality at Dunsink Observatory. I thank Dr. Ian Howarth for a preprint, and Dr. H. Lamers for detailed comments as referee. This work is supported in part by NASA Grant NAG 5-556.

References

Barker, P.K., Marlborough, J.I.: 1985, *Astrophys. J.*, 288, 329
Bruhweiler, F.: 1985 (private communication)
Burki, G., Heck, A., Bianchi, L., Cassatella, A.: 1982, *Astron. Astrophys.*, 107, 205
Garmany, C.D., Olson, G.L., Conti, P.S., Van Steenberg, M.E.: 1981, *Astrophys. J.*, 250, 660
Garmany, C.D., Conti, P.S.: 1984, *Astrophys. J.*, 284, 705
Gathier, R., Lamers, H., Snow, T.: 1981, *Astrophys. J.*, 247, 173 (GLS)
Grady, C. et al.: 1985, *Astron. Astrophys. Suppl.* (in press)
Gry, C., Lamers, H., Vidal-Madjar, A.: 1984, *Astron. Astrophys.*, 137, 29
Henrichs, H. et al.: 1980, Proc. *2nd Europen IUE Conf.* (ESA SP-157), p. 147
Henrichs, H.: 1984 in Proc. *Fourth European IUE Conference* (ESA SP-218), p. 43 (H84)
Holzer, T.E.: 1979, in *Solar System Plasma Physics*, eds. E.N. Parker, C.F. Kennel, L.J. Lanzerotti, North Holland, Amsterdam, Vol. 1, p. 101
Lamers, H., Gathier, R., Snow, T.P.: 1982, *Astrophys. J.*, 258, 186 (LGS)
Lamers, H., Korevaar, P., and Cassatella, A.: 1985, *Astron. Astrophys.*, 149, 29
Mullan, D.J.: 1984a, *Astrophys. J.*, 283, 303
Mullan, D.J.: 1984b, *Astrophys. J.*, 284, 769
Pecker, J.C.: 1982, in Stalio (1982), p. 270

Pizzo, V.J.: 1983, in *Solar Wind Five*, ed. M. Neugebauer, NASA Conf. Publ. 2280, p. 675
Praderie, F., Catala, C., Czarny, J., Felenbok, P.: 1984, in *Space Research Prospects in Stellar Activity and Varibility*, eds. A. Mageney and F. Praderie, Observ. Paris-Meudon, p. 265
Prinja, R.K. and Howarth, I.D.: 1984, *Astron. Astrophys.*, **133**, 110
Prinja, R.K. and Howarth, I.D.: 1985, preprint (PH)
Snow, T. and Morton D.C.: 1976, *Astrophys. J. Suppl.*, **217**, 760
Stalio, R. (editor): 1982, *Observational Basis for Velocity Fields in Stellar Atmospheres*, pp. 261–275
Vogt, S.S., Penrod, G.D.: 1983, *Astrophys. J.*, **275**, 661
Walborn, N., Panek, R.: 1984, *Astrophys. J. Letts.*, **280**, L27

D.J. Mullan: Displaced narrow absorption components
D.J. Mullan: Displaced narrow absorption components
D.J. Mullan: Displaced narrow absorption components
D.J. Mullan: Displaced narrow absorption components
D.J. Mullan: Displaced narrow absorption components
D.J. Mullan: Displaced narrow absorption components
D.J. Mullan: Displaced narrow absorption components